A Three-Dimensional Physical Model of MRI Noise Based on Current Noise Sources in a Conductor

Michael J. Hennessy

Intermagnetics General Corporation, Latham, New York 12110

Magnetic flux noise is generated by any conductor in equilibrium with a bath as a result of random fluctuating currents. A physical model of this flux noise is proposed, based on allowable current patterns in the conductor, which we describe as natural current modes. This model gives insight into the spatial characteristics of the magnetic noise which is encountered in a variety of magnetic measurements and imaging modalities such as magnetic resonance imaging (MRI). © 2000 Academic Press

Key Words: magnetic resonance imaging; signal-to-noise ratio; magnetic flux noise; current noise; high-temperature superconducting RF coils.

INTRODUCTION

With the advent of high-temperature superconducting RF coils, there is a pressing need to understand the underlying noise sources in magnetic resonance imaging (MRI). Superconductors have made it possible to obtain more perfect MRI noise images from patients without the interference of noise from the RF coil. The same is true for nuclear magnetic resonance (NMR) applications and other applications requiring the detection of magnetic flux.

Historically, models describing the noise detected from conducting bodies commonly invoke the reciprocity theorem. This approach was introduced by Hoult *et al.* (*1, 2*) to explain the signal-to-noise ratio in NMR and MRI. In this method, the noise resistance is computed indirectly from the loading of the detection coil as if it were a transmitter. The idea underlying this approach is reciprocity between detection and transmission, i.e., the source resistance of a detector coil is equated to the load resistance of an equivalent circuit in which the detector is used as a transmitter. This is a convenient tool for computing the response of a given coil geometry, but it does little for understanding the noise patterns underlying the detection coils. We suggest an alternative method, a more fundamental approach using three-dimensional current noise sources. This method is an expansion of previous work (*3, 4*).

PHYSICAL DESCRIPTION

For simplicity, we begin by considering a homogeneous conductor which is electrically isolated from external current

sources but is in thermal equilibrium with a bath. In the source-based picture, flux noise in this conductor arises from randomly fluctuating noise currents. Random noise currents are movements of charge forming a dissipation which is in equilibrium with the bath.

We have some limited knowledge of these currents. First of all, the currents are confined to the conductor. Mathematically, one can use this information to express the current as a series of orthogonal spatial functions. A key part of the physical model is the realization that the series of spatial functions correspond to natural current modes, each having a distinct pattern. In the source-based picture, each individual current mode is assigned an amplitude which varies randomly in time. Collectively, these currents form the composite fluctuating current. The spatial dependence of the natural current modes depends primarily on the sample shape and geometry. Each mode is independent of the other and represents a single degree of freedom for the current.

Another consequence of the currents being confined inside the conductor is the requirement that the current density at any instant may not enter or exit on any part of the surface of the conductor. While this may be viewed an obvious requirement, it imposes restrictions on the allowable current paths. This, combined with electrical isolation (no externally applied voltage sources within or on the surface of the conductor), forces the noise current to flow in closed loops, solenoidal in nature.

In addition to the obvious restrictions on the spatial dependence, there are restrictions on the time dependence of the currents as well. Although noise currents are random, we have some knowledge of their average intensity, which is apportioned by thermal equilibrium. Each mode is in thermal equilibrium since it represents a degree of freedom in the system. Knowledge of the intensity and spatial dependence of random noise currents is all that is required to evaluate noise level detected by any flux sensitive detector. The currents generate fluctuating fields and magnetic flux which can be computed directly from Maxwell's equations.

THE NATURE OF CURRENT NOISE

We begin the analysis by assuming the noise current density resides inside the conductor. The conductor is assumed to be

electrically isolated with no externally applied scalar potentials at or near the conductor. We also assume there are no appreciable displacement currents inside or outside the conductor. These assumptions are consistent with the so-called "quasi-static" approximation for electrically isolated conductive materials, which have $((\omega\epsilon)/\sigma) \ll 1$. (In the case of whole body MRI this applies for frequencies below 64 MHz.) With these restrictions, the noise current cannot build up charge nor escape at any point on the surface. Consequently, the noise current density normal to the surface of the conductor vanishes, so that,

$$\mathbf{J} \cdot \hat{\mathbf{n}} = 0, \qquad [1]$$

where $\hat{\mathbf{n}}$ is normal to the surface and $\mathbf{J}$ is the noise current density. The noise currents are physical currents, which means they must obey the continuity relation given by,

$$\nabla \cdot \mathbf{J} + \frac{\partial \rho}{\partial t} = 0. \qquad [2]$$

Because we have assumed the conductor is uniform and electrically isolated, there are no charge sources or sinks in the conductor. This means there is no change in charge, so that the divergence of the current must be zero, hence

$$\nabla \cdot \mathbf{J} = 0. \qquad [3]$$

VECTOR NOISE SOURCE ($\vec{\psi}$)

Since the divergence of the current density is zero, there exists a generating vector function $\vec{\psi}$, such that

$$\mathbf{J} = \nabla \times \vec{\psi}. \qquad [4]$$

In this context, $\vec{\psi}$ automatically satisfies the divergence equation, Eq. [3], since the divergence of the curl of any vector function is zero. We seek a realistic set of solutions $\vec{\psi}$ which satisfies the boundary conditions. As a consequence, this means that not all spatial behavior is acceptable. The finite boundaries of the conductor "filters" out some solutions.

The function $\vec{\psi}$ can be interpreted physically as a magnetization density, as a current stream function, or as an electric vector potential. These are all equivalent interpretations (5, 6). In the context of our application, we prefer to view $\vec{\psi}$ as the fundamental noise source, a source stream function which generates current density noise. The current density noise is of primary interest here because we can investigate the dissipation and the fields generated by it. We assume the current density noise source, $\vec{\psi}$, is a white vector noise source, a function whose amplitude, phase, and direction varies randomly in time. One way of describing $\vec{\psi}$ is to define it in terms of three
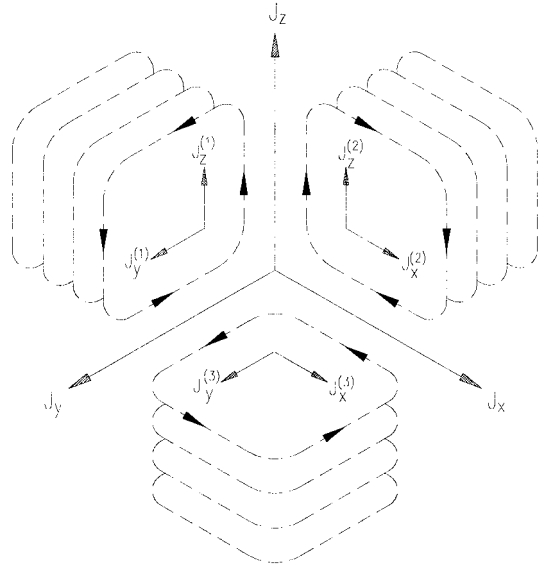

FIG. 1.   The decomposition of three-dimensional current density into three independent two-dimensional parts. The source $\psi^{(1)}$ is in the x direction and generates $J_y^{(1)}$ and $J_z^{(1)}$. The circular current loops near $J_y^{(1)}$ and $J_z^{(1)}$ are typical of those created by $\psi^{(1)}$. Current densities and current loops are also shown for the other orthogonal sources $\psi^{(2)}$ and $\psi^{(3)}$.

independent random variables. In the Cartesian coordinates, one can represent $\vec{\psi}$ as

$$\vec{\psi} = \psi^{(1)}\hat{\mathbf{x}} + \psi^{(2)}\hat{\mathbf{y}} + \psi^{(3)}\hat{\mathbf{z}}. \qquad [5]$$

Each component is a scalar noise source, uncorrelated and independent of the other. The concept of expressing $\vec{\psi}$ in terms of three scalar noise sources is valid in any orthogonal coordinate system. For the Cartesian coordinate system, we see that each component of $\vec{\psi}$ produces two components of current density given by

$$\mathbf{J}^{(1)} = \nabla \times [\psi^{(1)}\hat{\mathbf{x}}] \qquad [6]$$

$$\mathbf{J}^{(2)} = \nabla \times [\psi^{(2)}\hat{\mathbf{y}}] \qquad [7]$$

$$\mathbf{J}^{(3)} = \nabla \times [\psi^{(3)}\hat{\mathbf{z}}]. \qquad [8]$$

These currents are two-dimensional in nature and lie in a plane perpendicular to the source, as shown in Fig. 1. For example, $\psi^{(1)}$ generates only y–z currents which circulate about the $\hat{\mathbf{x}}$ axis. The total current density noise is the sum of all the two-dimensional current densities and is given by

$$\mathbf{J} = \sum_{\nu=1}^{3} \mathbf{J}^{(\nu)}. \qquad [9]$$

The noise current consists of a superposition of three two-dimensional currents which are independent and uncorrelated

with one another since they are formed from independent noise sources. This decomposition allows us to reduce the three-dimensional current density noise into three sets of less complex two-dimensional current densities, each driven by an independent scalar noise source.

THE CONCEPT OF NOISE SOURCE MODES

Because the noisy region exists only in the conductor and the conductor is bounded, each component of the stream function and associated current densities can be decomposed physically into a sum of spatially independent modes. At any given time, the spatial "boundedness" allows one to expand any component of $\vec{\psi}$ as a series of discrete orthogonal spatial functions which are identified as modes (7). For example, the x component of the source function can be expanded into an infinite series of modes,

$$\psi^{(1)} = \sum_{\eta} a_{\eta}^{(1)}(t)\varphi_{\eta}(x, y, z), \qquad [10]$$

where, φ_{η} is the orthogonal spatial function of the ηth mode. The amplitude $a_{\eta}^{(1)}(t)$ is a randomly fluctuating function representing the strength of the ηth mode at a given time. The total noise current associated with the **x** directed stream function is a sum over modes and is given by

$$\mathbf{J}^{(1)} = \sum_{\eta} \mathbf{J}_{\eta}^{(1)}, \qquad [11]$$

where

$$\mathbf{J}_{\eta}^{(1)} = \nabla \times \hat{\mathbf{x}} a_{\eta}^{(1)}(t)\varphi_{\eta}(x, y, z). \qquad [12]$$

CURRENT NOISE INTENSITY

The noise picked up by RF coils or flux sensors in MRI measurements is thermally driven magnetic noise from the sample itself. For the model, we assume for simplicity that the MRI sample is a conductor with a resistivity ρ and is in equilibrium with a bath near room temperature. For MRI applications, the noise power spectrum G is independent of frequency over the measurement bandwidth and is given by the Nyquist relation, which can be expressed simply as,

$$G = 4kT. \qquad [13]$$

The fluctuating power associated with black body radiation over a given bandwidth Δf is simply

$$P = 4kT\Delta f. \qquad [14]$$

On the other hand, time-averaged dissipated power associ-

ated with the fluctuation of a current density spatial mode η from a given source component ν at a frequency f is given by

$$P_d = \left\langle \rho \int \int \int \left| \mathbf{J}_{\eta}^{\nu}(\mathbf{r}, t) \right|^2 dV \right\rangle. \qquad [15]$$

These powers are in equilibrium which allows us to write

$$\left\langle \rho \int \int \int \left| \mathbf{J}_{\eta}^{\nu}(\mathbf{r}, t) \right|^2 dV \right\rangle = 4kT\Delta f. \qquad [16]$$

Thermal equilibrium is isotropic here, with no preference in noise source direction ν. [In Ref. (8), the Nyquist relation, which has been recast in Eq. [16], is derived using the methods of Kubo. The equilibrium condition with blackbody radiation is sometimes described in statistical mechanics as the fluctuation dissipation theorem.]

The power P_d represents the power dissipated by the source, assuming no loads are connected to the source. This is Joule heating due to the source currents alone. It also represents the maximum available power which can be delivered to external circuits. There is also Joule heating due to eddy currents. The current noise sources induce a minuscule amount of eddy currents in the conductor. In this case, the conductor itself acts as an "external circuit." The source currents magnetically couple to the conductor which appear as a load. Eddy current dissipation does not play a role in partitioning the available noise power in the conductor, because eddy currents are load currents rather than source currents. Eddy currents develop via inductive coupling and shield the magnetic fields generated by noise currents, giving rise to a penetration or skin depth effect.

RELATIONSHIP BETWEEN CURRENT DENSITY NOISE AND RF COIL FLUX

Noise in a conductor appears as time-dependent fluctuating current densities which act as field sources, inducing magnetic flux and generating a voltage which can be detected by a detector coil or RF receiver coil. (Here we assume the RF coil consists of perfect conductors and does not generate any additional noise in the detection process.) The fluctuating current density and its associated fields also generate eddy currents in the conductor, which tend to shield the flux. This can easily be seen from Maxwell's equations involving the noise current density $\mathbf{J}_{noise}$,

$$\nabla \times \mathbf{B} = \mu(\mathbf{J}_{noise} + \mathbf{J_e}) \qquad [17]$$

$$\nabla \times \mathbf{E} = -\frac{\partial \mathbf{B}}{\partial t} \qquad [18]$$

$$\nabla \cdot \mathbf{B} = 0 \tag{19}$$

$$\nabla \cdot \mathbf{E} = 0. \tag{20}$$

In Eq. [17] we assume a quasi-static behavior where currents are flowing through a homogeneous conductor with negligible displacement currents. The eddy current $\mathbf{J}_e$ induced by the noise current is given through Ohm's Law,

$$\mathbf{J}_e = \sigma \mathbf{E}. \tag{21}$$

In this analysis we assume the conductivity σ is independent of frequency, which is usually valid within the bandwidth of the measurement.

Since the divergence of $\mathbf{B}$ is zero, we introduce the vector potential $\mathbf{A}$,

$$\nabla \times \mathbf{A} = \mathbf{B}. \tag{22}$$

Substituting Eq. [22] into Maxwell's equation [17] and also into Ohm's law, we obtain the differential equation for the vector potential inside the conductor in terms of the noise current density,

$$-\nabla^2 \mathbf{A}^{in} + \mu \sigma \frac{\partial \mathbf{A}^{in}}{\partial t} = \mu \mathbf{J}_{noise}. \tag{23}$$

The time dependence of the vector potential generates an electric field since,

$$\mathbf{E} = -\nabla V - \frac{\partial \mathbf{A}}{\partial \mathbf{t}}.$$

In this analysis, we have selected the Coulomb gauge $(\nabla \cdot \mathbf{A} = 0)$ and since there are no voltage sources, the static potential V is zero or constant both inside and outside the conductor and does not contribute to the formation of fields or currents. Consequently, the induced currents are eddy currents and are given by

$$\mathbf{J}_e = -\sigma \frac{\partial \mathbf{A}^{in}}{\partial t}. \tag{24}$$

The eddy currents are not primary source currents, but rather secondary "load currents," currents resulting from the changing fields generated by the source currents. Outside the conductor, the vector potential obeys a slightly different equation,

$$-\nabla^2 \mathbf{A}^{out} = \mu_o (\mathbf{J}_{noise} + \mathbf{J}_e). \tag{25}$$

In a typical flux-detection measurement, a coil is used as a detector and it is placed about the sample. The flux induced in a detector coil is given in terms of the vector potential as,

$$\Phi(t) = \oiint_{coil} \mathbf{B}(\mathbf{r},\, t) \cdot \mathbf{dS} = \oint_{coil} \mathbf{A}(\mathbf{r},\, \mathbf{t}) \cdot \mathbf{dl}. \tag{26}$$

The analysis clearly demonstrates that the flux noise picked up in an RF coil is driven by current density noise through the vector potential. The exact form of the vector potential depends on whether the RF coil lies inside or outside the sample.

NOISE IN THE RF COIL

The relationship between current density noise, flux noise, and detectable voltage noise in an RF coil can be found by starting from the definition of mean squared flux, which is given by

$$\Phi_{rms}^2 \equiv \lim_{T \to \infty} \frac{1}{T} \int_{-T/2}^{T/2} \Phi^2(t)\,dt. \tag{27}$$

Moving from time to frequency, we define the Fourier frequency components $\Phi(\omega)$ as

$$\Phi(t) = \int_{-\infty}^{\infty} \Phi(\omega)\exp(i\omega t)\,d\omega, \tag{28}$$

and where

$$\Phi(\omega) = \frac{1}{2\pi} \int_{-\infty}^{\infty} \Phi(t)\exp(i\omega t)\,dt. \tag{29}$$

For MRI applications one is usually interested in a relatively narrow band of frequencies centered about the resonant frequency (ω_o). Assuming the flux noise spectrum $\Phi(\omega)$ is fairly constant over a bandwidth Δf centered at ω_o, the root mean squared flux in the time domain is given by

$$\Phi_{rms}^2 = (2\pi)^2 \Delta f |\Phi(\omega_o)|^2. \tag{30}$$

For an RF coil detector, a single-turn or multiturn loop is formed around the region of interest. The voltage measured across a single-turn RF coil is the time derivative of the induced flux which leads to

$$|V(\omega_o)|^2 = \omega_o^2 |\Phi(\omega_o)|^2. \tag{31}$$

In a similar manner, one can relate the rms voltage to the voltage power spectrum $|V(\omega)|^2$ in

$$V_{rms}^2 = (2\pi)^2 \Delta f |V(\omega_o)|^2. \quad [32]$$

The voltage power spectrum is normally measured in MRI and it is related to the flux power spectrum in

$$V_{rms}^2 = (2\pi)^2 \Delta f \omega_o^2 |\Phi(\omega_o)|^2. \quad [33]$$

At this stage, it is common to express the noise in terms of an equivalent noise resistance seen by the RF coil. In this instance, the noise resistance of a perfect lossless RF coil is defined through the Nyquist relation,

$$V_{rms}^2 = 4kT\Delta f R_{noise}. \quad [34]$$

Comparing the voltage noise associated with flux in Eq. [33] to the usual Nyquist formula, the equivalent noise resistance of an RF coil can be identified as

$$R_{noise} = \frac{\pi^2 \omega_o^2}{kT} |\Phi(\omega_o)|^2, \quad [35]$$

where

$$\Phi(\omega_o) = \oiint_{coil} \mathbf{B}(\mathbf{r}, \omega_o) \cdot \mathbf{dS} \quad [36]$$

and

$$\mathbf{B}(\mathbf{r}, \omega_o) = \frac{1}{2\pi} \int_{-\infty}^{\infty} \mathbf{B}(\mathbf{r}, t)\exp(i\omega_o t)dt. \quad [37]$$

We can also identify the noise resistance associated with a particular spatial current mode. Since the currents and fields of each mode are uncorrelated, the flux from each mode is also uncorrelated. This leads to a form valid in any orthogonal coordinate system,

$$R_{noise} = \sum_{\nu=1}^{3} \sum_{\eta} R_{\eta}^{(\nu)}, \quad [38]$$

where

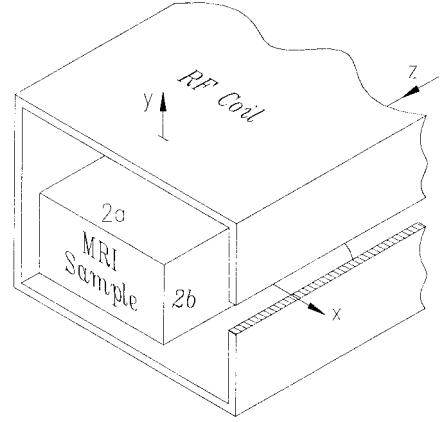$$R_{\eta}^{(\nu)} = \frac{\pi^2 \omega_o^2}{kT} |\Phi_{\eta}^{(\nu)}(\omega_o)|^2, \quad [39]$$

FIG. 2. Two-dimensional rectangular sample and RF coil configuration. The RF coil and sample are infinitely long in the z direction.

in which $\Phi_{\eta}^{(\nu)}(\omega_o)$ is the flux generated by the νth scalar noise source component and the ηth spatial mode. For the Cartesian case, the noise resistance has separate contributions from x, y, z noise source stream functions.

TWO-DIMENSIONAL NOISE SOURCES IN A RECTANGULAR CONDUCTOR

As a simple demonstration of the source-based methodology, we consider the case of a long rectangular conductor with uniform conductivity. This conductor has dimensions 2a and 2b and a very long length 2L shown in Fig. 2. Since the conductor is extremely long in the z direction, we can neglect end effects, which means the source and its associated currents are independent of z. This reduces to a two-dimensional problem with the stream function in the z direction, generating noise currents only in the x–y plane. Because the current is bounded within a rectangular region in the x–y plane, the stream function over this region can be expanded into a Fourier series, which is given by

$$\psi_z = \psi^{(3)} = \sum_{l=1}^{l=\infty} \sum_{m=1}^{m=\infty} \sum_{p=0}^{p=1} \sum_{q=0}^{q=1}$$
$$\times \psi_{lm,pq}^{(3)}(t)\cos(k_l x + \phi_p)\cos(k_m y + \phi_q), \quad [40]$$

where the discrete spatial frequencies are defined as

$$k_l = \frac{l\pi}{2a}, \quad k_m = \frac{m\pi}{2b}, \quad \text{where } l, m = 1, 2, 3\ldots,$$
$$[41]$$

and the integers l, m identify the mode pattern and the phases ϕ_p, ϕ_q are in phase and out of phase components so that

$$\phi_p = \frac{p\pi}{2} \qquad \text{and} \qquad \phi_q = \frac{q\pi}{2}. \qquad [42]$$

This notation is a compact way of representing the conventional two-dimensional Fourier series which contains all combinations of sines and cosines. The function $\psi_{lm,pq}^{(3)}(t)$ is the amplitude of the noise source stream function for a specific current density mode or pattern. The corresponding current densities are derived from the curl of $\psi^{(3)}$, which become

$$J_x^{(3)}(x, y, t) = -\sum_{l=1}^{l=\infty} \sum_{m=1}^{m=\infty} \sum_{p=0}^{p=1} \sum_{q=0}^{q=1}$$

$$\times k_m \psi_{lm,pq}^{(3)}(t)\cos(k_l x + \phi_p)\sin(k_m y + \phi_q) \qquad [43]$$

$$J_y^{(3)}(x, y, t) = +\sum_{l=1}^{l=\infty} \sum_{m=1}^{m=\infty} \sum_{p=0}^{p=1} \sum_{q=0}^{q=1}$$

$$\times k_l \psi_{lm,pq}^{(3)}(t)\sin(k_l x + \phi_p)\cos(k_m y + \phi_q). \qquad [44]$$

To meet the boundary condition $\mathbf{J} \cdot \hat{\mathbf{n}} = 0$ at the surface, only certain modes are allowed, including

$$\begin{aligned}
\cos(k_l x) &\quad \text{for } l = odd \text{ and } p = 0; \\
\sin(k_l x) &\quad \text{for } l = even \text{ and } p = 1; \\
\cos(k_m y) &\quad \text{for } m = odd \text{ and } q = 0; \\
\sin(k_m y) &\quad \text{for } m = even \text{ and } q = 1.
\end{aligned}$$

This provides a rich mixture of harmonics for generating random patterns, collectively forming current loops of all imaginable sizes and shapes. In Figs. 3 and 4 we show examples of allowable current patterns which fit the boundary conditions. Note that the even/odd current patterns in Fig. 4 contribute no flux in the *x–y* plane and are hence invisible to any flux detector which encompasses the boundary of the conductor. It is evident that only odd cosine harmonics, such as those shown in Fig. 3, contribute flux to the RF coil.

The vector current density associated with each mode can now be fully described using Eqs. [43] and [44]. Following the notation in Eq. [8] we have

$$\mathbf{J}_{lm,pq}^{(3)}(\mathbf{r}, t) = -\psi_{lm}^{(3)}(t)[k_m \hat{\mathbf{x}} \cos(k_l x + \phi_p)\sin(k_m y + \phi_q)$$

$$+ k_l \hat{\mathbf{y}} \sin(k_l x + \phi_p)\cos(k_m y + \phi_q)]. \qquad [45]$$

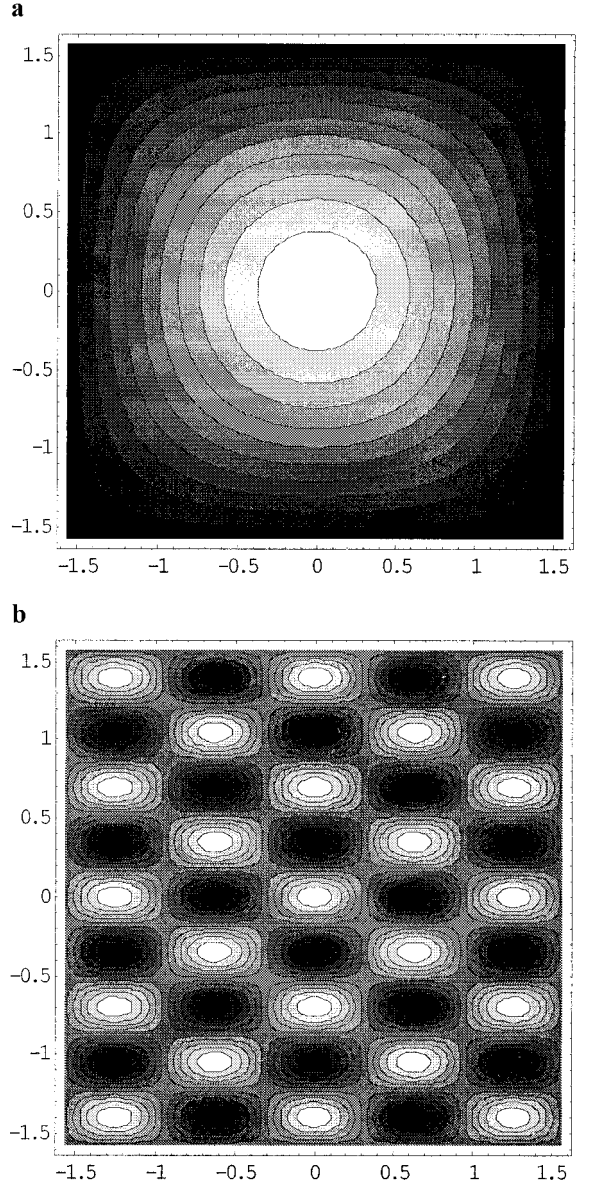At this stage, the intensity of the noise source can be found

FIG. 3. Odd, odd current density modes: (a) contour plot of the lowest order current density noise source mode $l = 1$, $m = 1$ in a rectangular conductor or MRI sample, (b) contour plot of the current density noise source mode $l = 5$, $m = 9$ in a rectangular conductor or MRI sample. The current is flowing clockwise in the bright region and counterclockwise in the dark region. The noise current density amplitude of a given mode is random in time but flows in the same pattern.

from thermal equilibrium described in Eq. [16], which expands into

$$\rho\langle|\psi_{lm,pq}^{(3)}(t)|^2\rangle \int_{-a}^{a} dx \int_{-b}^{b} dy \int_{-L}^{L} dz$$

$$\times [k_m^2\cos^2(k_l x + \phi_p)\sin^2(k_m y + \phi_q)$$

$$+ k_l^2\sin^2(k_l x + \phi_p)\cos^2(k_m y + \phi_q)] = 4kT\Delta f. \qquad [46]$$
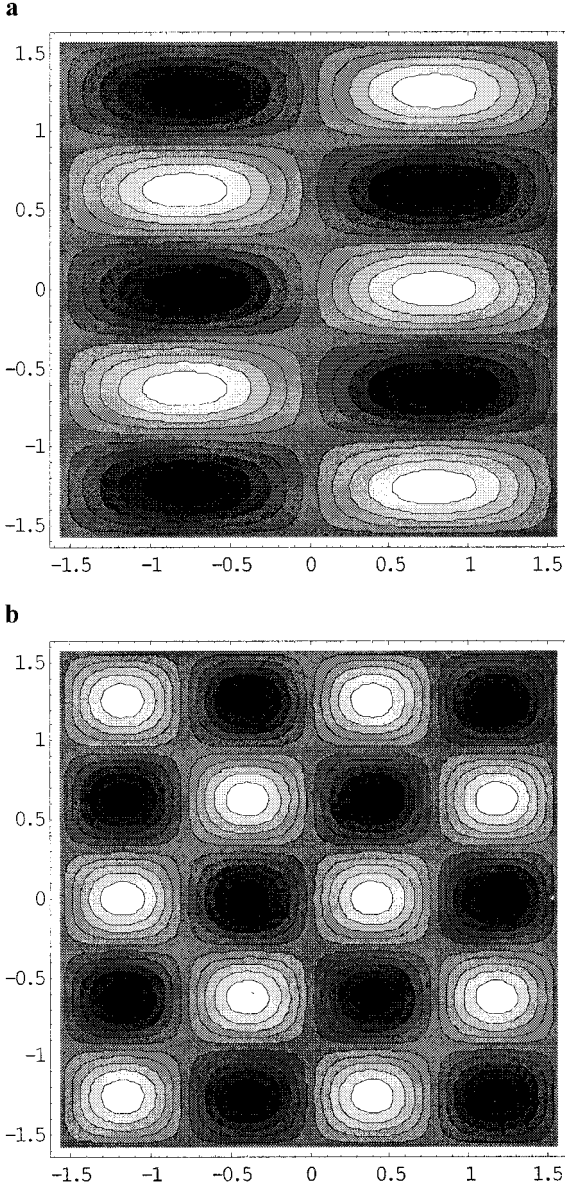
a

b

FIG. 4. Even, odd current density modes: (a) contour plot of current density noise mode $l = 2$ $m = 5$, (b) contour plot of current density noise mode $l = 4$ $m = 5$. The current is flowing clockwise in the bright region and counterclockwise in the dark region. An RF coil would have no net flux generated by these current density patterns because there is the same number of current loops flowing clockwise and counterclockwise.

Integrating on the left side, the expression reduces to

$$\langle |\psi_{lm,pq}^{(3)}(t)|^2 \rangle = \frac{4kT\Delta f}{\rho k_{lm}^2 ab(2L)},$$ [47]

where

$$k_{lm}^2 = k_l^2 + k_m^2.$$ [48]

The next step in the analysis is to examine the magnetic fields and flux generated by the noise currents. The magnetic fields associated with the noise currents are most naturally derived from the magnetic vector potential in the conductor. Because the conductor is bounded, the vector potential can be expanded into Fourier components, which are given by

$$\mathbf{A}(\mathbf{r}, t) = \sum_{l,m;p,q} \mathbf{A}_{lm,pq}(\mathbf{r}, t),$$ [49]

where

$$\mathbf{A}_{lm,pq}(\mathbf{r}, t) = A_{lm}^x(t)\hat{\mathbf{x}} \cos(k_l x + \phi_p)\cos(k_m y + \phi_q)$$
$$+ A_{lm}^x(t)\hat{\mathbf{y}} \cos(k_l x + \phi_p)\cos(k_m y + \phi_q).$$ [50]

Moving from the time domain to the frequency domain,

$$\psi_{lm,pq}^{(3)}(\mathbf{r}, \omega) = \frac{1}{2\pi}\int_{-\infty}^{\infty}\psi_{lm,pq}^{(3)}(\mathbf{r}, \omega)\exp(i\omega t)dt$$ [51]

$$\mathbf{J}_{lm,pq}^{(3)}(\mathbf{r}, \omega) = \frac{1}{2\pi}\int_{-\infty}^{\infty}\mathbf{J}_{lm,pq}^{(3)}(\mathbf{r}, t)\exp(i\omega t)dt$$ [52]

$$\mathbf{A}_{lm,pq}(\mathbf{r}, \omega) = \frac{1}{2\pi}\int_{-\infty}^{\infty}\mathbf{A}_{lm,pq}(\mathbf{r}, t)\exp(i\omega t)dt.$$ [53]

Solving for the vector potential Fourier components using Eqs. [49] and [23], the solution becomes

$$\mathbf{A}_{lm,pq}(\mathbf{r}, \omega) = \frac{\mu\mathbf{J}_{lm,pq}^{(3)}(\mathbf{r}, \omega)}{-k_{lm}^2 + i\omega\mu\sigma}.$$ [54]

Matching like terms leaves

$$A_{lm,pq}^x(\omega) = \frac{-\mu k_m}{-k_{lm}^2 + i\omega\mu\sigma}\psi_{lm,pq}^{(3)}(\omega)$$ [55]

and

$$A_{lm,pq}^y(\omega) = \frac{-\mu k_l}{-k_{lm}^2 + i\omega\mu\sigma}\psi_{lm,pq}^{(3)}(\omega).$$ [56]

The complete vector field function associated with a given mode is then

$$\mathbf{A}_{lm,pq}(\mathbf{r},\,\omega) = \frac{-\mu\psi_{lm,pq}^{(3)}(\omega)}{-k_{lm}^2 + i\omega\mu\sigma}$$
$$\times\,[k_m\hat{\mathbf{x}}\cos(k_l x + \phi_p)\sin(k_m y + \phi_q)$$
$$+\,k_l\hat{\mathbf{y}}\,\sin(k_l x + \phi_p)\cos(k_m y + \phi_q)].$$

[57]

To find the magnetic field in the conductor, one uses the curl of the vector potential in Eq. [22], which results in

$$\mathbf{B}_{lm}(\omega) = \mu\psi_{lm,pq}^{(3)}(\omega)\,\frac{-k_{lm}^2\hat{\mathbf{z}}}{-k_{lm}^2 + i\omega\mu\sigma}$$
$$\times\,\cos(k_l x + \phi_p)\cos(k_m y + \phi_p).$$

[58]

Integrating this over the region defined by the RF coil, one has the magnetic flux, which is given by

$$\Phi_{lm}(\omega_o) = \oiint_{coil} \mathbf{B}_{lm}(\mathbf{r},\,\omega_o)\cdot d\mathbf{S}.$$

[59]

For the case where the RF coil encloses only the region of the conductor

$$\Phi_{lm,pq}(\omega) = \mu\psi_{lm,pq}^{(3)}(\omega)\,\frac{-k_{lm}^2}{-k_{lm}^2 + i\omega\mu\sigma}\int_{-a}^{a} dx \int_{-b}^{b} dy$$
$$\times\,\cos(k_l x + \phi_p)\cos(k_m y + \phi_q),$$

[60]

which becomes

$$\Phi_{lm,pq}(\omega) = \mu\psi_{lm,pq}^{(3)}(\omega)\,\frac{-4k_{lm}^2}{k_l k_m(-k_{lm}^2 + i\omega\mu\sigma)}$$
$$\times\,\sin\left(\frac{l\pi}{2}\right)\sin\left(\frac{m\pi}{2}\right)\cos(\phi_p)\cos(\phi_q).$$

[61]

A net noise flux only exists for odd l, m and $p = q = 0$, which is obvious when examining the current density patterns in Fig. 3. This means the stream function noise and the flux noise consist of only cosine terms with odd l and m. It is interesting to note that the flux noise and the stream function noise or, equivalently, the noise magnetization have similar spatial patterns.

The noise resistance of the mode can be obtained from the noise flux using Eq. [39] with the only surviving terms being

$$R_{lm} = \frac{\pi^2\omega_o^2}{kT}\,|\Phi_{lm,00}(\omega_o)|^2$$

[62]

or

$$R_{lm} = \frac{\pi^2\omega_o^2}{kT}\,|\psi_{lm,00}^{(3)}(\omega_o)|^2\,\frac{16\mu^2}{k_l^2 k_m^2}\,\frac{k_{lm}^4}{k_{lm}^4 + (\omega_o\mu\sigma)^2}.$$

[63]

Substituting the known mean squared intensity of the noise source, we have the corresponding spectral density from Eq. [47],

$$\langle|\psi_{lm,00}^{(3)}(t)|^2\rangle = 4\pi^2\Delta f|\psi_{lm,00}^{(3)}(\omega_o)|^2$$
$$= \frac{4kT\Delta f}{\rho(k_l^2 + k_m^2)ab(2L)}.$$

[64]

This simplifies into

$$|\psi_{lm,00}^{(3)}(\omega_o)|^2 = \frac{kT}{\pi^2 k_{lm}^2 ab(2L)}.$$

[65]

Putting this into the formula for noise resistance, Eq. [63], the noise resistance can be written

$$R_{lm} = \frac{64\mu^2\omega_o^2}{\rho(2a2b)(2L)}\,\frac{1}{k_l^2 k_m^2}\,\frac{k_{lm}^2}{k_{lm}^4 + (\omega_o\mu\sigma)^2}.$$

[66]

We can associate a characteristic mode frequency for each mode defined as

$$\omega_{lm} = \frac{k_l^2 + k_m^2}{\mu\sigma}.$$

[67]

So that

$$R_{lm} = R_{lm}^o\,\frac{\left(\dfrac{\omega_o}{\omega_{lm}}\right)^2}{1 + \left(\dfrac{\omega_o}{\omega_{lm}}\right)^2},$$

[68]

where

$$R_{lm}^o = \frac{64\rho}{V}\left[\left(\frac{2a}{l\pi}\right)^2 + \left(\frac{2b}{m\pi}\right)^2\right],$$

[69]

and where V is the volume of the sample. The total noise becomes a sum over all modes,
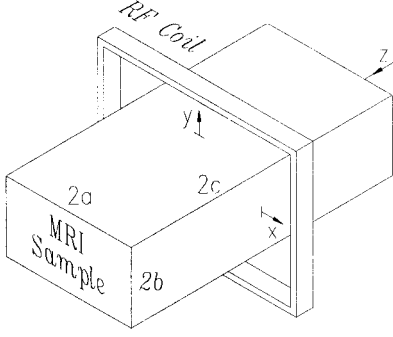
$$R_{noise} = \sum_{l,m\,odd} R_{lm}.$$

[70]

FIG. 5. Three-dimensional rectangular sample and RF coil configuration. The RF coil and sample have different lengths in the *z* direction.

The same expression can be derived using reciprocity methods as shown in Appendix I, but the interpretation of the formula is different and it is not obvious that the modes correspond to specific noise patterns. In the reciprocity calculation, the dissipated power is caused by induced eddy current patterns generated in the sample when the RF coil is used as a transmitter. The total load or noise resistance is formed by summing the power dissipation per unit amp caused by each eddy current pattern. This means we can associate the transmitter driven eddy current patterns with the actual spatial noise sources.

THREE-DIMENSIONAL NOISE IN A RECTANGULAR CONDUCTOR

As an example of a three-dimensional noise source, we examine a conductor shown in Fig. 5. Because it is bounded in three dimensions, the noise source can be described as a series of three-dimensional orthogonal stream functions given by

$$\psi_x = \psi^{(1)} = \sum_{l=0}^{l=\infty} \sum_{m=0}^{m=\infty} \sum_{n=0}^{n=\infty} \sum_{p=0}^{p=1} \sum_{q=0}^{q=1} \sum_{r=0}^{r=1} \psi^{(1)}_{lmn,pqr}(t)$$

$$\times \cos(k_l x + \phi_p)\cos(k_m x + \phi_q)\cos(k_n x + \phi_r) \quad [71]$$

$$\psi_y = \psi^{(2)} = \sum_{l=0}^{l=\infty} \sum_{m=0}^{m=\infty} \sum_{n=0}^{n=\infty} \sum_{p=0}^{p=1} \sum_{q=0}^{q=1} \sum_{r=0}^{r=1} \psi^{(2)}_{lmn,pqr}(t)$$

$$\times \cos(k_l x + \phi_p)\cos(k_m x + \phi_q)\cos(k_n x + \phi_r) \quad [72]$$

$$\psi_z = \psi^{(3)} = \sum_{l=0}^{l=\infty} \sum_{m=0}^{m=\infty} \sum_{n=0}^{n=\infty} \sum_{p=0}^{p=1} \sum_{q=0}^{q=1} \sum_{r=0}^{r=1} \psi^{(3)}_{lmn,pqr}(t)$$

$$\times \cos(k_l x + \phi_p)\cos(k_m x + \phi_q)\cos(k_n x + \phi_r). \quad [73]$$

Here we have discrete *k* values which are readily identified in the vector

$$\mathbf{k}_{lmn} = \frac{l\pi}{2a}\,\hat{\mathbf{x}} + \frac{m\pi}{2b}\,\hat{\mathbf{y}} + \frac{n\pi}{2c}\,\hat{\mathbf{z}} = k_l\hat{\mathbf{x}} + k_m\hat{\mathbf{y}} + k_n\hat{\mathbf{z}} \quad [74]$$

and the phases

$$\phi_p = \frac{p\pi}{2} \qquad \phi_q = \frac{q\pi}{2} \qquad \phi_r = \frac{r\pi}{2}, \quad [75]$$

where *l*, *m*, *n*, *p*, *q*, and *r* are positive integers. The corresponding noise current densities derived from the stream functions are

$$\mathbf{J}^{(1)} = \sum \psi^{(1)}_{lmn,pqr}(t)\cos(k_l x + \phi_p)$$

$$\times \, [-ik_n\hat{\mathbf{y}}\cos(k_m y + \phi_q)\sin(k_n z + \phi_r)$$

$$+ \, ik_m\hat{\mathbf{z}}\sin(k_m y + \phi_q)\cos(k_n z + \phi_r)] \quad [76]$$

$$\mathbf{J}^{(2)} = \sum \psi^{(2)}_{lmn,pqr}(t)\cos(k_m y + \phi_q)$$

$$\times \, [ik_n\hat{\mathbf{x}}\cos(k_l x + \phi_p)\sin(k_n z + \phi_r)$$

$$- \, ik_l\hat{\mathbf{z}}\sin(k_l x + \phi_p)\cos(k_n z + \phi_r)] \quad [77]$$

$$\mathbf{J}^{(3)} = \sum \psi^{(3)}_{lmn,pqr}(t)\cos(k_n z + \phi_r)$$

$$\times \, [-ik_m\hat{\mathbf{x}}\cos(k_l x + \phi_p)\sin(k_m y + \phi_q)$$

$$+ \, ik_l\hat{\mathbf{y}}\sin(k_l x + \phi_p)\cos(k_m y + \phi_q)]. \quad [78]$$

As before, the boundary condition requires that the normal component of the noise current vanish at the surface, so that only certain stream function harmonics are allowed. The allowable harmonics are

$$\begin{aligned}
\cos(k_l x) & \quad \text{for } l = odd \text{ and } p = 0; \\
\sin(k_l x) & \quad \text{for } l = even \text{ and } p = 1; \\
\cos(k_m y) & \quad \text{for } m = odd \text{ and } q = 0; \\
\sin(k_m y) & \quad \text{for } m = even \text{ and } q = 1; \\
\cos(k_n z) & \quad \text{for } n = odd \text{ and } r = 0; \\
\sin(k_n z) & \quad \text{for } n = even \text{ and } r = 1.
\end{aligned}$$

The time-averaged noise intensities can be found by applying the conditions of black body radiation in Eq. [17], from which we find

$$\langle |\psi^{(1)}_{lmn,pqr}(t)|^2 \rangle = \frac{4kT\Delta f}{\rho k^2_{mn}abc} \quad [79]$$

$$\langle |\psi^{(2)}_{lmn,pqr}(t)|^2 \rangle = \frac{4kT\Delta f}{\rho k^2_{ln}abc} \quad [80]$$

$$\langle|\psi_{lmn,pqr}^{(3)}(t)|^2\rangle = \frac{4kT\Delta f}{\rho k_{lm}^2 abc}, \qquad [81]$$

where

$$k_{mn}^2 = k_m^2 + k_n^2 \qquad [82]$$

$$k_{\text{ln}}^2 = k_l^2 + k_n^2 \qquad [83]$$

$$k_{lm}^2 = k_l^2 + k_m^2. \qquad [84]$$

It is interesting to note that the surviving intensities are independent of the phase, specifically the phase variables p, q, and r. The vector potentials from each source can be derived from Maxwell's equations using Eq. [23] and are given by

$$\mathbf{A}_{lmn,pqr}^{(1)}(\mathbf{r}, \omega) = \frac{-\mu\psi_{lmn,pqr}^{(1)}(t)}{-k_{lmn}^2 + i\mu\sigma\omega} \cos(k_l x + \phi_p)$$
$$\times [-k_n \hat{\mathbf{y}} \cos(k_m y + \phi_q)\sin(k_n z + \phi_r)$$
$$+ k_m \hat{\mathbf{z}} \sin(k_m y + \phi_q)\cos(k_n z + \phi_r)]$$
$$[85]$$

$$\mathbf{A}_{lmn,pqr}^{(2)}(\mathbf{r}, \omega) = \frac{-\mu\psi_{lmn,pqr}^{(2)}(t)}{-k_{lmn}^2 + i\mu\sigma\omega} \cos(k_m y + \phi_q)$$
$$\times [k_n \hat{\mathbf{x}} \cos(k_l x + \phi_p)\sin(k_n z + \phi_r)$$
$$- k_l \hat{\mathbf{z}} \sin(k_l x + \phi_p)\cos(k_n z + \phi_r)]$$
$$[86]$$

$$\mathbf{A}_{lmn,pqr}^{(3)}(\mathbf{r}, \omega) = \frac{-\mu\psi_{lmn,pqr}^{(3)}(t)}{-k_{lmn}^2 + i\mu\sigma\omega} \cos(k_n z + \phi_r)$$
$$\times [-k_m \hat{\mathbf{x}} \cos(k_l x + \phi_p)\sin(k_m y + \phi_q)$$
$$+ k_l \hat{\mathbf{y}} \sin(k_l x + \phi_p)\cos(k_m y + \phi_q)].$$
$$[87]$$

From the geometry of the RF coil shown in Fig. 1, the magnetic field of interest is in the $\hat{\mathbf{z}}$ direction, normal to the plane of the RF coil. The z-component of the magnetic field is derived from the curl of the vector potential, and is given by,

$$B_z = \frac{\partial A_y}{\partial x} - \frac{\partial A_x}{\partial y}. \qquad [88]$$

Separating the magnetic field into parts associated with each scalar noise source, we have

$$\mathbf{B}_{lmn,pqr}^{(1)}(\omega) = \frac{-\mu k_l k_n \psi_{lmn,pqr}^{(1)}(\omega)}{-k_{lmn}^2 + i\omega\mu\sigma} \cos(k_l x + \phi_p)$$
$$\times \sin(k_m y + \phi_q)\sin(k_n z + \phi_r)\hat{\mathbf{z}} + \ldots \quad [89]$$

$$\mathbf{B}_{lmn,pqr}^{(2)}(\omega) = \frac{-\mu k_m k_n \psi_{lmn,pqr}^{(2)}(\omega)}{-k_{lmn}^2 + i\omega\mu\sigma} \sin(k_l x + \phi_p)$$
$$\times \cos(k_m y + \phi_q)\sin(k_n z + \phi_r)\hat{\mathbf{z}} + \ldots \quad [90]$$

$$\mathbf{B}_{lmn,pqr}^{(3)}(\omega) = \frac{-\mu k_{lm}^2 \psi_{lmn,pqr}^{(3)}(\omega)}{-k_{lmn}^2 + i\omega\mu\sigma} \cos(k_l x + \phi_p)$$
$$\times \cos(k_m y + \phi_q)\cos(k_n z + \phi_r)\hat{\mathbf{z}} + \ldots \quad [91]$$

We proceed to solve the flux in the RF coil, which is given by

$$\Phi_{lmn,pqr}(\omega) = \oiint_{coil} [\mathbf{B}_{lmn,pqr}^{(1)}(\omega) + \mathbf{B}_{lmn,pqr}^{(2)}(\omega)$$
$$+ \mathbf{B}_{lmn}^{(3)}(\omega)] \cdot \hat{\mathbf{z}}dxdy. \qquad [92]$$

Grouping the flux by noise components, we have

$$\Phi_{lmn,pqr}^{(1)}(\omega)$$
$$= \mu\psi_{lmn,pqr}^{(1)}(\omega)\cos[k_n z + \phi_r] \frac{-k_l k_n}{-k_{lmn}^2 + i\omega\mu\sigma}$$
$$\times \int_{-a}^{a} dx \int_{-b}^{b} dy \cos(k_l x + \phi_p)\sin(k_m y + \phi_q) \quad [93]$$

$$\Phi_{lmn,pqr}^{(2)}(\omega)$$
$$= \mu\psi_{lmn,pqr}^{(2)}(\omega)\cos[k_n z + \phi_r] \frac{-k_m k_n}{-k_{lmn}^2 + i\omega\mu\sigma}$$
$$\times \int_{-a}^{a} dx \int_{-b}^{b} dy \sin(k_l x + \phi_p)\cos(k_m y + \phi_q) \quad [94]$$

$$\Phi_{lmn,pqr}^{(3)}(\omega)$$
$$= \mu\psi_{lmn,pqr}^{(3)}(\omega)\cos[k_n z + \phi_r] \frac{-k_{lm}^2}{-k_{lmn}^2 + i\omega\mu\sigma}$$
$$\times \int_{-a}^{a} dx \int_{-b}^{b} dy \cos(k_l x + \phi_p)\cos(k_m y + \phi_q). \quad [95]$$

The noise resistance is related to the sum of the flux power spectra of each component, which is written

$$R_{lmn} = \frac{\pi^2\omega_o^2}{kT} \sum_{\nu=1}^{3} |\Phi_{lmn,pqr}^{(\nu)}(\omega_o)|^2. \qquad [96]$$

In Appendix B, we show that for a thin coil located at $z = 0$, the noise resistance becomes

$$R_{lmn} = \mu^2 \frac{\pi^2 \omega_o^2}{kT} \frac{16kT}{\rho \pi^2 abc[k_{lmn}^4 + (\omega_o \mu \sigma)^2]}$$

$$\times \left(\frac{k_n^2}{k_m^2 k_{mn}^2} + \frac{k_n^2}{k_l^2 k_{ln}^2} \right) \sin^2\left(\frac{l\pi}{2}\right) \sin^2\left(\frac{m\pi}{2}\right) \text{for } n \text{ even}$$

[97]

and,

$$R_{lmn} = \mu^2 \frac{\pi^2 \omega_o^2}{kT} \frac{16kT}{\rho \pi^2 abc[k_{lmn}^4 + (\omega_o \mu \sigma)^2]}$$

$$\times \left(\frac{1}{k_l^2} + \frac{1}{k_l^2} \right) \sin^2\left(\frac{l\pi}{2}\right) \sin^2\left(\frac{m\pi}{2}\right) \text{for } n \text{ odd.}$$

[98]

This can be rearranged so that the MRI noise resistance of a single spatial mode becomes

$$R_{lmn} = R_{lmn}^o \frac{\dfrac{\omega_o^2}{\omega_{lmn}^2}}{\left[1 + \left(\dfrac{\omega_o}{\omega_{lmn}} \right)^2 \right]},$$

[99]

where the characteristic frequencies are defined as

$$\omega_{lmn} = \frac{k_{lmn}^2}{\mu \sigma}.$$

[100]

The frequency independent parts are segregated into odd and even parts, where

$$R_{lmn}^o = \frac{16\rho}{abc} \left(\frac{k_n^2}{k_m^2 k_{mn}^2} + \frac{k_n^2}{k_l^2 k_{ln}^2} \right) \sin^2\left(\frac{l\pi}{2}\right) \sin^2\left(\frac{m\pi}{2}\right) \; n \text{ odd,}$$

[101]

$$R_{lmn}^o = \frac{16\rho}{abc} \left(\frac{1}{k_l^2} + \frac{1}{k_m^2} \right) \sin^2\left(\frac{l\pi}{2}\right) \sin^2\left(\frac{m\pi}{2}\right) \; n \text{ even.}$$ [102]

The total MRI noise resistance for the 3D rectangular is the sum over all modes, which is

$$R_{noise} = \sum_{l,m,n} R_{lmn}.$$

[103]

The noise consists of terms generated by the z directed stream function $\psi^{(1)}$ and also includes contributions from $\psi^{(2)}$ and $\psi^{(3)}$. The coil "feels" the noise from the x–y sources through the k_n dependence which originates from $\psi^{(2)}$ and $\psi^{(3)}$.

To verify that three-dimensional noise resistance can be reduced to that of the 2D model, we examine the limiting case

of a long sample. We show in Appendix B that as $c \rightarrow L$, where L is large,

$$k_n = \frac{n\pi}{2c} \rightarrow 0,$$ [104]

from which follows

$$\omega_{lmn} \rightarrow \omega_{lm}$$ [105]

and

$$\sum_n R_{lmn} \rightarrow R_{lm}^o \frac{\left(\dfrac{\omega_o}{\omega_{lm}} \right)^2}{1 + \left(\dfrac{\omega_o}{\omega_{lm}} \right)^2}.$$ [106]

This agrees with the noise resistance of the two-dimensional model in Eq. [68].

RESULTS

Noise detected in NMR and MRI is a combination of noise generated by the RF coil, the sample, and the RF preamplifiers. (For MRI, the sample noise is normally called patient or body noise.) The noise of an ideal instrument is dominated by the sample noise. Other noise sources are usually minimized by using high-Q RF coils and low-noise preamplifiers. It has been known *a priori* that the origin of the sample noise is randomly fluctuating currents in the sample.

Sample noise is physically Johnson noise associated with the sample's source resistance. Noise is usually described as a single scalar parameter with no indication of its spatial dependence. In this work we have shown that noise can be expressed as a three-dimensional current noise source and is related to the temperature and resistivity of the sample. Maxwell's equations restrict the allowable current patterns in any bounded conductive sample. Only certain distinct current patterns (current density modes) are allowed to exist in a bounded conductor. This restriction also applies to noise current sources. The total noise current consists of a vector sum of these normal modes having randomly fluctuating amplitudes. This makes the noise source current appear as if it were flowing in random paths through the conductor. An example of noise current density patterns predicted by the two-dimensional model are shown in Figs. 6 and 7 for various instances in time.

Current noise generates joule heating which is in thermal equilibrium with the bath. Because of the equilibrium condition between the bath temperature and the dissipation, one is able to quantify the time-averaged intensity of each independent current density mode. Each current density mode generates a fluctuating magnetic field. The fluctuating field produces
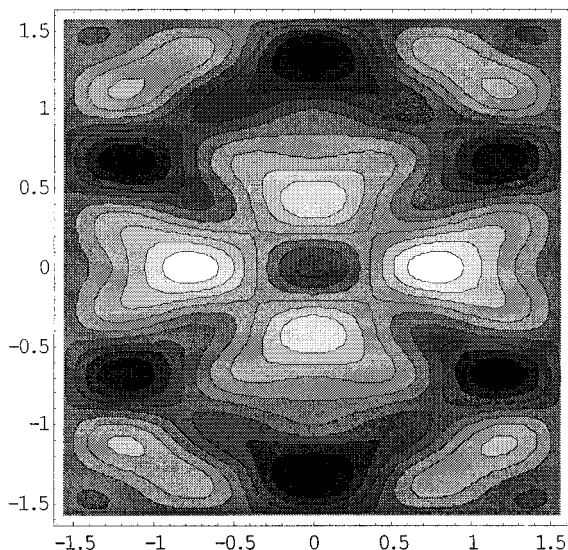
FIG. 6. A composite current density noise source with mode content up to $l = 5$, $m = 9$ containing only odd harmonics. The pattern represents a snapshot of the random current density in a rectangular MRI phantom as it might appear at a given time. The symmetry is due to the presence of only odd harmonics.

flux noise. Flux noise from the noise currents in the sample or patient generates a voltage in RF coils, which is the "body noise" detected in MRI.

A quasi-static model has been developed in this work which gives a simple physical picture of imaged noise sources. The noise resistance computed from the model for a two-dimensional rectangular sample agrees with the reciprocity methods. It is found that for any given geometry the noise predicted by the source-based approach is not different from that derived from reciprocity. Reciprocity is a fundamentally sound approach for evaluating noise, as long as the system behaves in a linear fashion. The focus of reciprocity is usually a single scalar result like noise resistance. What is different about the source-based approach is that information about the spatial distribution of the noise naturally flows out of the analysis.

The current is decomposed into spatial modes fluctuating independently from one another. The current modes can be thought of as localized k space modes in the sample. The analysis shows that MRI noise is not evenly distributed in k-space. This should not be surprising, particularly if we visualize a "perfect MRI noise image." In a perfect MRI noise image, magnetic noise should appear only where noise is generated. Furthermore, the noise image should have a contrast associated with its conductivity and temperature; i.e., regions of high conductivity generate more noise since the noise resistance is proportional to the conductivity as demonstrated in Eqs. [97] and [98]. Most MRI techniques do not form true noise images or images which reflect the true location and contrast of the noise sources. Instead, most

MRI techniques evenly spread the noise all over k-space, which results in noise spreading throughout all regions of image space, including regions were no sample exists. Noise spillover is very obvious in human imaging. Regions of high conductivity (for example muscle) should be noisier than those of low conductivity (for example fat). This is not usually observed in MRI images.

The source of this phenomena can be traced to the way images are normally acquired in MRI. The signal spatial information is encoded and mixed with a composite noise signal consisting of noise coming from all regions of the sample. The noise is not encoded spatially, so information about its location is lost in the acquisition process. In most methods, noise is allowed to leak in uniformly over k-space, whereas the real noise source is not constant in k-space. A true k-space noise image would have projections or profiles which would have no noise beyond the boundary of the sample and a noise intensity which follows the shape of the object. The leaking phenomena makes the noise image appear much different than it actually is. In many MRI images, the noise image appears uniform over the FOV, whereas in reality it should be confined to the noise source region.

One method of presenting a more realistic noise picture is by restricting the FOV. If the FOV is restricted only to a volume containing the conductive material, the noise outside the FOV disappears. This can be accomplished by restricting the size of the RF coil or simply by truncating the image at the known boundaries of the conductor. Truncation forces the noise to zero in those regions which are known to be void of conductive material. Truncation in space is a form of filtering which removes spatially miscoded k-space noise responsible for gen-
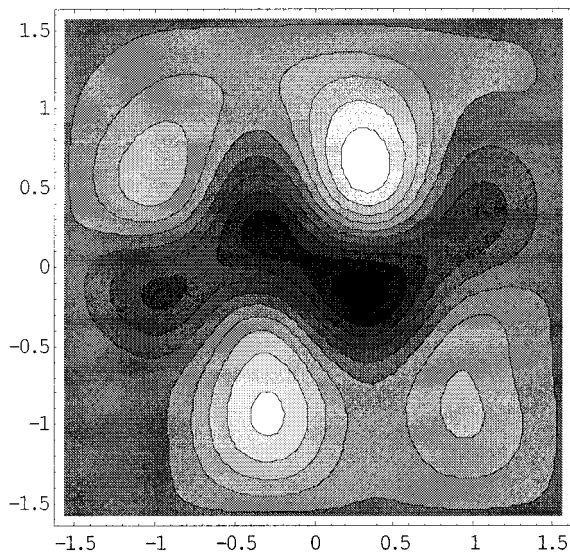

FIG. 7. A composite current density noise source with mode content up to $l = 8$ $m = 9$ containing odd and even harmonics. The pattern represents a snapshot of the random current density as it might appear in a rectangular MRI phantom. Note the pattern looks random and has no symmetry.

erating noise in void regions. This is a brute force approach. Other techniques combine the use of RF coil arrays (such as SMASH and SENSE) and are more spatially selective, providing an opportunity for the display of a more realistic distribution of noise in k-space.

CONCLUSIONS

Two- and three-dimensional models have been developed to explain the behavior of MRI/NMR noise sources which fall within the quasi-static (low-frequency) regime. The two-dimensional form of the model has been shown to be in agreement with reciprocity, which has been well established experimentally and is routinely used to estimate RF noise attributed to the sample. The three-dimensional model converges to the two-dimensional model in the limit of long samples.

It is too early to predict exactly what new information will be gleaned from this model. Often times different views yield different insights which lead to new innovations. Take for example the role of equivalent networks and how powerful a given representation can be beyond the voltage and current it predicts. The source-based model gives an equivalent but new view of the origin and production of sample generated noise working its way into magnetic measurements. The model is not intended to be a routine tool to evaluate the performance of a given detector coil configuration which can readily be done by reciprocity and finite element analysis. Instead, the model presents for the first time a detailed picture of the intrinsic sample noise, a three-dimensional vector noise source, which, heretofore, has been lumped into a single scalar parameter such as noise resistance or noise voltage. The model is expected to be helpful in formulating and evaluating noise reduction strategies, especially in MRI systems.

APPENDIX A

Reciprocity Derivation for the Noise Resistance of a 2-D Rectangular Conductor

Assume the RF coil in the transmission mode consists of an infinitely long current sheet flowing around a rectangular sample as shown in Fig. 2. The field obeys Maxwell's quasi-static equations and Ohm's Law and is given by

$$\nabla \times \mathbf{B} = \mu(\mathbf{J}_d + \mathbf{J}_e)$$

$$\nabla \times \mathbf{E} = \frac{\partial \mathbf{B}}{\partial t}$$

$$\mathbf{J}_e = \sigma \mathbf{E}$$

$$\nabla \cdot \mathbf{J}_e = 0.$$

Here, $\mathbf{J}_d$ is the drive current in the RF coil and $\mathbf{J}_e$ is the eddy current developed in the sample. The current sheet is assumed
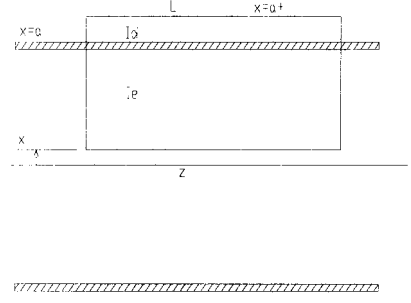

FIG. A1. Integration path for the two-dimensional noise model.

to be very thin, having a width of Δ. Following Fig. A1, the drive current density for this case can be written as,

$$\mathbf{J}_d = \lim_{\Delta \to 0} K\{\hat{\mathbf{x}}[\nu_+(x, a) - \nu_-(x, a)] + \hat{\mathbf{y}}[\nu(y, b)$$
$$- \nu(y, -b)]\}u(x, a + \Delta)u(y, b + \Delta), \quad [A1]$$

where

$\nu_+(\xi, a) = 1$ when $a < \xi < a + \Delta$ and zero otherwise,

$\nu_-(\xi, a) = 1$ when $-a < \xi < -a - \Delta$ and zero otherwise,

$u(\xi, a) = 1$ when $-a < \xi < a$ and zero otherwise.

There also exists an eddy current stream function such that,

$$\nabla \times \vec{\psi} = \mathbf{J}_e,$$

which satisfies the divergence

$$\nabla \cdot \mathbf{J}_e = \mathbf{0}.$$

Now the integration over a path shown in Fig. A1 is such that

$$\oiint_{a,b} \nabla \times \mathbf{B} \cdot \mathbf{dS} = \mu \oiint_{a,b} (\mathbf{J}_d + \mathbf{J}_e) \cdot \mathbf{dS} = \mu I_d + \mu I_e.$$
$$[A2]$$

Using Green's theorem, this reduces to the line integral

$$\oint \mathbf{B} \cdot \mathbf{dl} = \mu \oiint_{a,b} \mathbf{J}_d \cdot \mathbf{dS} + \oint \nabla \times \vec{\psi} \cdot \mathbf{dS} = \mu I_d + \mu I_e.$$
$$[A3]$$

Completing the integration

$$B_z(x, y) \cdot L = \mu K u(x, a) u(y, b) \cdot L$$
$$- \mu[\psi_z(x, y) - \psi_z(a_+, y)] \cdot L. \quad [A4]$$

Here we have taken the limit for a thin current sheet in the following integrals:

$$\oiint \mathbf{J}_d \cdot \mathbf{dS} = \lim_{\Delta \to 0} K \int_x^{a+} \int_0^L \{\hat{\mathbf{x}}[\nu_+(x, a) - \nu_-(x, a)]$$
$$+ \hat{\mathbf{y}}[\nu(y, b) - \nu(y, -b)]\}$$
$$\times u(x, a + \Delta) u(y, b + \Delta) \cdot \hat{\mathbf{y}} dx dz$$

$$\oiint \mathbf{J}_d \cdot \mathbf{dS} = \lim_{\Delta \to 0} K u(x, a + \Delta) u(y, b) \cdot L$$
$$= K u(x, a) u(y, b) \cdot L. \quad [A5]$$

Similarly in the *y–z* plane,

$$\oiint \mathbf{J}_d \cdot \mathbf{dS} = \lim_{\Delta \to 0} K u(x, a) u(y, b + \Delta) \cdot L$$
$$= K u(x, a) u(y, b) \cdot L. \quad [A6]$$

There is no eddy current beyond the conductor, consequently in this region, ψ should be a constant or zero. This means the magnetic field in the sample is related to the drive current and eddy currents in the material following Eq. [A3],

$$B_z(x, y) = \mu K u(x, a) u(y, b) - \mu\psi_z(x, y). \quad [A7]$$

Since the eddy currents are constrained inside a conductor, the stream function can be expressed in a Fourier series,

$$\psi_z = \sum_{lm,pq} \psi_{lm,pq} \cos(k_l x + \phi_p) \cos(k_m y + \phi_q). \quad [A8]$$

The current densities are derived from the curl of the steam function and are

$$J_{lm}^x = -k_m \psi_{lm}(t) \cos(k_l x + \phi_p) \sin(k_m y + \phi_q) \quad [A9]$$

$$J_{lm}^y = k_l \psi_{lm}(t) \sin(k_l x + \phi_l) \cos(k_m y + \phi_m), \quad [A10]$$

where

$$k_l = \frac{l\pi}{2a}, \quad k_m = \frac{m\pi}{2b}, \quad \text{and} \quad l, m = 1, 2, 3. \ldots, \quad [A11]$$

$$\phi_p = \frac{p\pi}{2} \quad \text{and} \quad \phi_q = \frac{q\pi}{2}. \quad [A12]$$

The integers *l*, *m* identify the mode pattern, and the phases ϕ_p, ϕ_q are adjusted to meet the boundary conditions. The changing magnetic field induces the eddy currents, since

$$\nabla \times \frac{\mathbf{J}_e}{\sigma} = \frac{\partial \mathbf{B}}{\partial t}. \quad [A13]$$

Putting in the sinusoidal dependence we have

$$i\sigma\omega B_z = \frac{\partial J_x}{\partial y} - \frac{\partial J_y}{\partial x}.$$

Substituting the current density in the above expression yields

$$i\sigma\omega B_z = -\sum_{lm} (k_l^2 + k_m^2)\psi_{lm,pq}$$
$$\times \cos(k_l x + \phi_p)\cos(k_m y + \phi_q), \quad [A14]$$

and since

$$B_z(x, y) = \mu K u(x, a)u(y, b) - \mu\psi_z(x, y), \quad [A15]$$

$$\sum_{lm,pq} (k_l^2 + k_m^2 + i\mu\sigma\omega)\psi_{lm,pq}\cos(k_l x + \phi_p)\cos(k_m y + \phi_q)$$
$$= i\mu\sigma\omega K u(x, a)u(y, b). \quad [A16]$$

The next step is to identify the stream function harmonics. This is easily done if we recognize that the harmonic content of the two-dimensional unit-bounded function can be expressed

$$u(x, a)u(y, b) = \frac{16}{\pi^2} \sum_{l,m \ odd} \frac{1}{lm} \cos(k_l x)\cos(k_m y). \quad [A17]$$

This implies that only the $p = 0$, $q = 0$ harmonics contribute and they are given by

$$\psi_{lm,00} = -\frac{i\mu\sigma\omega}{k_l^2 + k_l^2 + i\mu\sigma\omega} K_{lm}, \quad [A18]$$

where

$$K_{lm} = \frac{16K}{\pi^2} \frac{1}{lm} \qquad \text{where } l, m \text{ are odd and zero otherwise.}$$

[A19]

In the reciprocity argument, quantity of interest is the power loading or the power dissipated in the conductor. If we assume the conductor and RF coil extends from $z = -L$ to $+L$ the power dissipated is

$$P = \frac{1}{2}\rho \int \mathbf{J} \cdot \mathbf{J}^* d\nu = \frac{1}{2}\rho \sum_{l,m} \psi_{lm,00}^2 \int_{-c}^{c} \int_{-b}^{b} \int_{-a}^{a}$$
$$\times (k_l^2 \cos^2 k_l x \sin^2 k_m y + k_m^2 \cos^2 k_m x \sin^2 k_l y) dz\, dy\, dx.$$

[A20]

This reduces to

$$P = 256\rho(\mu\sigma\omega)^2 ab(2L) K^2$$
$$\times \sum_{l,m \text{ odd}} \frac{k_l^2 + k_m^2}{(k_l^2 + k_m^2)^2 + (\mu\sigma\omega)^2} \frac{1}{l^2 m^2 \pi^4}.$$

[A21]

The noise resistance is simply equal to the load resistance, which can be found from the dissipated power and rms drive current at the resonance frequency, which is given by

$$R_{noise} = R_{load} = \frac{P}{\left(\frac{1}{\sqrt{2}} I_d\right)^2} = \frac{2P}{(K \cdot 2L)^2}.$$

[A22]

This leads to

$$R_{lm} = \frac{64\sigma\mu^2\omega_o^2 ab}{(8abL)(k_l k_m)^2}$$
$$\times \frac{k_l^2 + k_m^2}{(k_l^2 + k_m^2)^2 + (\mu\sigma\omega_o^2)^2} \qquad \text{for } l, m \text{ odd}$$

[A23]

$$R_{lm} = \frac{64\sigma\mu^2\omega_o^2 ab}{(8abL)(k_l k_m)^2} \frac{k_{lm}^2}{k_{lm}^4 + (\mu\sigma\omega_o^2)^2} \qquad \text{for } l, m \text{ odd,}$$

[A24]

which agrees with Eq. [66], and where

$$R_{noise} = \sum_{l,m \text{ odd}} R_{lm}.$$

[A25]

QED.

APPENDIX B

The Noise Resistance for a 3-D Rectangular Conductor

The noise resistance is obtained by completing the integration for the flux in Eqs. [93], [94], [95],

$$\Phi_{lmn,pqr}^{(1)}(\omega) = \mu\psi_{lmn,pqr}^{(1)}(\omega)\frac{-4k_l k_n}{k_l k_m(-k_{lmn}^2 + i\omega\mu\sigma)}$$
$$\times \sin[k_n z + \phi_r]\sin\left(\frac{l\pi}{2}\right)\sin\left(\frac{m\pi}{2}\right)$$
$$\times \cos\phi_p \sin\phi_q$$

[B1]

$$\Phi_{lmn,pqr}^{(2)}(\omega) = \mu\psi_{lmn,pqr}^{(2)}(\omega)\frac{-4k_m k_n}{k_l k_m(-k_{lmn}^2 + i\omega\mu\sigma)}$$
$$\times \sin[k_n z + \phi_r]\sin\left(\frac{l\pi}{2}\right)\sin\left(\frac{m\pi}{2}\right)$$
$$\times \sin\phi_p \cos\phi_q$$

[B2]

$$\Phi_{lmn,pqr}^{(3)}(\omega) = \mu\psi_{lmn,pqr}^{(3)}(\omega)\frac{-4k_{lm}^2}{k_l k_m(-k_{lmn}^2 + i\omega\mu\sigma)}$$
$$\times \cos[k_n z + \phi_r]\sin\left(\frac{l\pi}{2}\right)\sin\left(\frac{m\pi}{2}\right)$$
$$\times \cos\phi_p \cos\phi_q.$$

[B3]

For a thin coil at $z = 0$, the surviving terms for each component of the flux are

$$\Phi_{lmn,011}^{(1)}(\omega) = \mu\psi_{lmn,011}^{(1)}(\omega)\frac{-4k_l k_n}{k_l k_m(-k_{lmn}^2 + i\omega\mu\sigma)}$$
$$\times \sin\left(\frac{l\pi}{2}\right)\sin\left(\frac{m\pi}{2}\right) \text{ n even}$$

[B4]

$$\Phi_{lmn,101}^{(2)}(\omega) = \mu\psi_{lmn,101}^{(2)}(\omega)\frac{-4k_m k_n}{k_l k_m(-k_{lmn}^2 + i\omega\mu\sigma)}$$
$$\times \sin\left(\frac{l\pi}{2}\right)\sin\left(\frac{m\pi}{2}\right) \text{ n even}$$

[B5]

$$\Phi_{lmn,000}^{(3)}(\omega) = \mu\psi_{lmn,000}^{(3)}(\omega)\frac{-4k_{lm}^2}{k_l k_m(-k_{lmn}^2 + i\omega\mu\sigma)}$$
$$\times \sin\left(\frac{l\pi}{2}\right)\sin\left(\frac{m\pi}{2}\right) \text{ n odd.}$$

[B6]

The power spectra of the flux components are given by

$$|\Phi_{lmn,011}(\omega)|^2 = \mu^2|\psi_{lmn,011}^{(3)}(\omega)|^2\frac{16k_l^2 k_n^2}{k_l^2 k_m^2[k_{lmn}^4 + (\omega\mu\sigma)^2]}$$
$$\times \sin^2\left(\frac{l\pi}{2}\right)\sin^2\left(\frac{m\pi}{2}\right) \text{ n even}$$

[B7]

$$|\Phi_{lmn,101}(\omega)|^2 = \mu^2 |\psi_{lmn,101}^{(2)}(\omega)|^2 \frac{16k_m^2 k_n^2}{k_l^2 k_m^2 [k_{lmn}^4 + (\omega\mu\sigma)^2]}$$

$$\times \sin^2\left(\frac{l\pi}{2}\right)\sin^2\left(\frac{m\pi}{2}\right) \text{ n even} \qquad [B8]$$

$$|\Phi_{lmn,000}(\omega)|^2 = \mu^2 |\psi_{lmn,000}^{(3)}(\omega)|^2 \frac{16k_{lm}^4}{k_l^2 k_m^2 [k_{lmn}^4 + (\omega\mu\sigma)^2]}$$

$$\times \sin^2\left(\frac{l\pi}{2}\right)\sin^2\left(\frac{m\pi}{2}\right) \text{ n odd.} \qquad [B9]$$

At this point we need to evaluate the power spectra of Eqs. [71], [72], [73] in terms of the rms values in Eq. [13],

$$|\psi_{lmn,011}^{(1)}(\omega)|^2 = \frac{1}{4\pi^2\Delta f}\langle|\psi_{lmn,011}^{(1)}(t)|^2\rangle = \frac{kT}{\rho\pi^2 k_{mn}^2 abc}$$

$$[B10]$$

$$|\psi_{lmn,101}^{(2)}(\omega)|^2 = \frac{1}{4\pi^2\Delta f}\langle|\psi_{lmn,101}^{(3)}(t)|^2\rangle = \frac{kT}{\rho\pi^2 k_{ln}^2 abc}$$

$$[B11]$$

$$|\psi_{lmn,000}^{(3)}(\omega)|^2 = \frac{1}{4\pi^2\Delta f}\langle|\psi_{lmn,000}^{(3)}(t)|^2\rangle = \frac{kT}{\rho\pi^2 k_{lm}^2 abc}.$$

$$[B12]$$

Evaluating the noise resistance at the resonance frequency, we find

$$R_{lmn} = \frac{\pi^2\omega_o^2}{kT}\sum_{\nu=1}^{3}|\Phi_{lmn,pqr}^{\nu}(\omega_o)|^2 \qquad [B13]$$

$$R_{lmn} = \mu^2 \frac{\pi^2\omega_o^2}{kT}\frac{16kT}{\rho\pi^2 abc[k_{lmn}^4 + (\omega_o^2\mu\sigma)^2]}$$

$$\times \left(\frac{k_{lm}^2}{k_l^2 k_m^2}\right)\sin^2\left(\frac{l\pi}{2}\right)\sin^2\left(\frac{m\pi}{2}\right) \text{ n odd} \qquad [B14]$$

$$R_{lmn} = \mu^2 \frac{\pi^2\omega_o^2}{kT}\frac{16kT}{\rho\pi^2 abc[k_{lmn}^4 + (\omega_o^2\mu\sigma)^2]}$$

$$\times \left(\frac{k_n^2}{k_m^2 k_{mn}^2} + \frac{k_n^2}{k_l^2 k_{ln}^2}\right)\sin^2\left(\frac{l\pi}{2}\right)\sin^2\left(\frac{m\pi}{2}\right) \text{ n even.}$$

$$[B15]$$

Here it is convenient to define

$$\omega_{lmn} = \frac{k_{lmn}^2}{\mu\sigma}. \qquad [B16]$$

Separating out the frequency independent parts, we have

$$R_{lmn}^o = \frac{16\rho}{abc}\left(\frac{k_n^2}{k_m^2 k_{mn}^2} + \frac{k_n^2}{k_l^2 k_{ln}^2}\right)\sin^2\left(\frac{l\pi}{2}\right)\sin^2\left(\frac{m\pi}{2}\right) \text{ n even}$$

$$[B17]$$

$$R_{lmn}^o = \frac{16\rho}{abc}\left(\frac{k_{lm}^2}{k_l^2 k_m^2}\right)\sin^2\left(\frac{l\pi}{2}\right)\sin^2\left(\frac{m\pi}{2}\right) \text{ n odd.} \qquad [B18]$$

With these definitions, we form a concise solution:

$$R_{lmn} = R_{lmn}^o \frac{\dfrac{\omega_o^2}{\omega_{lmn}^2}}{\left[1 + \left(\dfrac{\omega_o^2}{\omega_{lmn}}\right)^2\right]}. \qquad [B19]$$

Note we can look at the 2D current in the limit of a long conductor $c \to L$. Here we have

$$k_n = \frac{n\pi}{2c} \to 0. \qquad [B20]$$

In this limit we see that for a long sample, the time-averaged intensity given in Eqs. [81] and [B12] changes and becomes

$$\langle|\psi_{lmn}^{(3)}(t)|^2\rangle \to \frac{4kT\Delta f}{\rho k_{lm}^2 ab2L}, \qquad [B21]$$

leaving

$$R_{lmn}^\infty \to \frac{16\rho}{ab(2L)}\left(\frac{1}{k_l^2} + \frac{1}{k_m^2}\right)\sin^2\left(\frac{l\pi}{2}\right)\sin^2\left(\frac{m\pi}{2}\right) = R_{lm}^\infty$$

$$[B22]$$

and

$$\omega_{lmn} \to \omega_{lm}. \qquad [B23]$$

This agrees with the 2D case. The RF coil "feels" the noise from the $\hat{x}$ and $\hat{y}$ noise generators $\psi(1)$ and $\psi(2)$ through the spatial harmonics associated with k_n.

An alternative equivalent demonstration of the 2D limit can be derived starting from a finite RF coil. Assume the RF coil extends from $-c_o$ to c_o, with N_o turns per meter, the total flux induced sensed by the coils is

$$\bar{\Phi}_{lmn,pqr}(\omega) = N_o \int_{-c_0}^{c_0} \Phi_{lmn,pqr}(z, \omega)dz. \qquad [B24]$$

Incorporating this integration into the frequency independent part of the noise resistance, we have

$$R^o_{lmn} = N_t^2 \text{sinc}^2(k_n c_o) \frac{16\rho}{abc} \left(\frac{k_n^2}{k_m^2 k_{mn}^2} + \frac{k_n^2}{k_l^2 k_{ln}^2} \right)$$
$$\times \sin^2\left(\frac{l\pi}{2}\right) \sin^2\left(\frac{m\pi}{2}\right) \text{ even n} \qquad [B25]$$

$$R^o_{lmn} = N_t^2 \text{sinc}^2(k_n c_o) \frac{16\rho}{abc} \left(\frac{k_{lm}^2}{k_l^2 k_m^2} \right)$$
$$\times \sin^2\left(\frac{l\pi}{2}\right) \sin^2\left(\frac{m\pi}{2}\right) \text{ odd n.} \qquad [B26]$$

In these expressions, the total number of turns N_t comes from the definition of N_o in the expression

$$N_t = \int_{-c_0}^{c_o} N_o dz = 2c_o N_o. \qquad [B27]$$

For the 2D model, $c \rightarrow L$ so that $k_n \rightarrow 0$ and $\omega_{lmn} \rightarrow \omega_{lm}$ and the mode intensity is reduced by $\frac{1}{2}$ as described in Eq. [47] because the z dependence is removed. This results in

$$R_{noise} = N_t^2 \sum_{l,m \text{ odd}} \frac{16\rho}{ab2L} \left(\frac{1}{k_l^2} + \frac{1}{k_m^2} \right) \frac{\frac{\omega_o^2}{\omega_{lm}^2}}{\left[1 + \left(\frac{\omega_o^2}{\omega_{lm}} \right)^2 \right]}.$$
$$[B28]$$

Incorporating the volume of the conductor we have

$$R_{noise} = N_t^2 \sum_{l,m \text{ odd}} \frac{64\rho}{V} \left(\frac{1}{k_l^2} + \frac{1}{k_m^2} \right) \frac{\frac{\omega_o^2}{\omega_{lm}^2}}{\left[1 + \left(\frac{\omega^2}{\omega_{lm}} \right)^2 \right]}.$$
$$[B29]$$

For a single turn, this reduces to the 2D expression in Eq. [68]. QED

REFERENCES

1. D. I. Hoult and R. E. Richards, The signal-to-noise ratio of the nuclear magnetic resonance experiment, *J. Magn. Reson.* **24,** 71 (1976).

2. D. I. Hoult and P. C. Lauterbur, The sensitivity of zeugmatographic experiment involving human samples, *J. Magn. Reson.* **34,** 425 (1979).

3. M. J. Hennessy and H. B. Zou, *Proc. SMR,* 1484 (1997).

4. M. J. Hennessy, *Proc. ISMRM,* 2049 (1999).

5. D. K. Cheng, "Field and Wave Electromagnetics," Addison–Wesley, New York (1992).

6. W. R. Smythe, "Static and Dynamic Electricity," 3rd ed., McGraw–Hill, New York (1968).

7. Churchill, R. V., "Fourier Series and Boundary Value Problems," McGraw–Hill, New York (1941).

8. G. H. Wannier, "Statistical Physics," Wiley, New York (1966).